



# Computation of Wave Loads under Multidirectional Sea States for Floating Offshore Wind Turbines

## Preprint

T. Duarte  
*EDP Inovação*

S. Gueydon  
*MARIN*

J. Jonkman  
*National Renewable Energy Laboratory*

A. Sarmiento  
*IST, University of Lisbon*

*To be presented at the 33<sup>rd</sup> International Conference on Ocean,  
Offshore and Arctic Engineering  
San Francisco  
June 8 – 13, 2014*

**NREL is a national laboratory of the U.S. Department of Energy  
Office of Energy Efficiency & Renewable Energy  
Operated by the Alliance for Sustainable Energy, LLC**

This report is available at no cost from the National Renewable Energy  
Laboratory (NREL) at [www.nrel.gov/publications](http://www.nrel.gov/publications).

**Conference Paper**  
NREL/CP-5000-61161  
March 2014

Contract No. DE-AC36-08GO28308

## NOTICE

The submitted manuscript has been offered by an employee of the Alliance for Sustainable Energy, LLC (Alliance), a contractor of the US Government under Contract No. DE-AC36-08GO28308. Accordingly, the US Government and Alliance retain a nonexclusive royalty-free license to publish or reproduce the published form of this contribution, or allow others to do so, for US Government purposes.

This report was prepared as an account of work sponsored by an agency of the United States government. Neither the United States government nor any agency thereof, nor any of their employees, makes any warranty, express or implied, or assumes any legal liability or responsibility for the accuracy, completeness, or usefulness of any information, apparatus, product, or process disclosed, or represents that its use would not infringe privately owned rights. Reference herein to any specific commercial product, process, or service by trade name, trademark, manufacturer, or otherwise does not necessarily constitute or imply its endorsement, recommendation, or favoring by the United States government or any agency thereof. The views and opinions of authors expressed herein do not necessarily state or reflect those of the United States government or any agency thereof.

This report is available at no cost from the National Renewable Energy Laboratory (NREL) at [www.nrel.gov/publications](http://www.nrel.gov/publications).

Available electronically at <http://www.osti.gov/scitech>

Available for a processing fee to U.S. Department of Energy and its contractors, in paper, from:

U.S. Department of Energy  
Office of Scientific and Technical Information  
P.O. Box 62  
Oak Ridge, TN 37831-0062  
phone: 865.576.8401  
fax: 865.576.5728  
email: <mailto:reports@adonis.osti.gov>

Available for sale to the public, in paper, from:

U.S. Department of Commerce  
National Technical Information Service  
5285 Port Royal Road  
Springfield, VA 22161  
phone: 800.553.6847  
fax: 703.605.6900  
email: [orders@ntis.fedworld.gov](mailto:orders@ntis.fedworld.gov)  
online ordering: <http://www.ntis.gov/help/ordermethods.aspx>

*Cover Photos: (left to right) photo by Pat Corkery, NREL 16416, photo from SunEdison, NREL 17423, photo by Pat Corkery, NREL 16560, photo by Dennis Schroeder, NREL 17613, photo by Dean Armstrong, NREL 17436, photo by Pat Corkery, NREL 17721.*



Printed on paper containing at least 50% wastepaper, including 10% post consumer waste.

# Computation of Wave Loads under Multidirectional Sea States for Floating Offshore Wind Turbines

**Tiago Duarte**  
EDP Inovação  
Lisboa, Portugal

**Jason Jonkman**  
National Renewable Energy Laboratory  
Golden, Colorado, USA

**Sébastien Gueydon**  
MARIN  
Netherlands

**António Sarmento**  
IST, University of Lisbon  
Lisboa, Portugal

## ABSTRACT

This paper focuses on the analysis of a floating wind turbine under multidirectional wave loading. Special attention is given to the different methods used to synthesize the multidirectional sea state. This analysis includes the double-sum and single-sum methods, as well as an equal-energy discretization of the directional spectrum. These three methods are compared in detail, including the ergodicity of the solution obtained. From the analysis, the equal-energy method proved to be the most computationally efficient while still retaining the ergodicity of the solution. This method was chosen to be implemented in the numerical code FAST. Preliminary results on the influence of these wave loads on a floating wind turbine showed significant additional roll and sway motion of the platform.

**Keywords:** Multidirectional Waves, Floating Wind Turbine, Synthesis of Multidirectional Seas.

## NOMENCLATURE

$S(\omega)$	frequency spectrum
$D(\theta)$	directional spectrum
$N$	number of discrete frequencies
$\Theta$	number of discrete directions
$\zeta(x, y, t)$	wave elevation at point $(x, y)$ and time $t$
$X(\omega, \theta)$	first-order load response amplitude operator
$X^{+/-}$	second-order load response amplitude operator (quadratic transfer function)

## 1. INTRODUCTION

Floating wind turbines are a promising technology to generate clean, renewable energy and are currently being studied with complex aero-hydro-servo-elastic modeling tools. Contributions from wave loads on the floating platform are most often modeled assuming unidirectional wave fields. However, the different wave components that comprise an irregular sea state come from different directions. Figure 1 compares the wave elevation obtained in the unidirectional case with a case involving multidirectional waves.

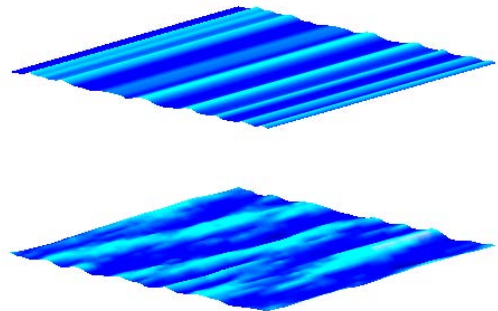


Figure 1. Unidirectional (top) versus multidirectional sea surface (bottom), under a JONSWAP spectrum, with  $H_s=6$  m,  $T_p=10$  s,  $\gamma=2.2$ , and the spreading factor  $s=2$ .

When modeling multidirectional sea states, the wave elevation is now a function not only of the wave frequency but also of the

incoming wave direction. In irregular waves, this is usually described with a directional spectrum or spreading function, similar to a frequency spectrum. It is assumed that the total spectrum can be defined as:

$$S(\omega, \theta) = S(\omega) \cdot D(\theta) \quad (1)$$

where  $S(\omega)$  is the frequency spectrum, independent of the direction of the waves, and  $D(\theta)$  is the directional spectrum. There are several ways to define the directional spectrum. The most commonly used is a cosine spreading function:

$$D(\theta) = C \left| \cos \left( \frac{\pi(\theta - \bar{\theta})}{2\theta_{max}} \right) \right|^{2s}, \quad \bar{\theta} - \theta_{max} < \theta < \bar{\theta} + \theta_{max} \quad (2)$$

where  $\theta$  is the incoming wave direction,  $\bar{\theta}$  is the mean wave direction,  $\theta_{max}$  is the maximum deviation from the mean wave direction, and  $s$  is the wave spreading parameter.  $C$  is a normalizing constant that is defined as [1]:

$$C = \frac{\sqrt{\pi}\Gamma(s+1)}{2\theta_{max}\Gamma(s+1/2)} \quad (3)$$

where  $\Gamma$  is the gamma function. This ensures that:

$$\int_{-\theta_{max}}^{\theta_{max}} D(\theta) d\theta = 1 \quad (4)$$

This is a very important property that must be fulfilled by every method used to compute the discrete spectrum (see Section 2.2). It guarantees that the total energy in each frequency band  $\Delta\omega$  is kept faithful to the frequency spectrum  $S(\omega)$ .

The direction spectrum can also be a function of frequency, if the spreading coefficient is set to be frequency dependent. Despite being the most common directional spectrum, other methods have been developed as an alternative to the  $\cos^{2s}$  spectrum. Reference [2] describes several of these methods, which are also included in the MatLab toolbox WAFO [3].

## 2. SYNTHESIS OF MULTIDIRECTIONAL SEAS

The water surface elevation at a given point  $(x, y)$  on the still water plane at a given instant  $t$  as a result of a regular progressive wave can be described simply by:

$$\zeta(x, y, t) = \text{Re}(Ae^{j(\omega t - K(x \cos(\theta) + y \sin(\theta)))}) \quad (5)$$

where  $A$  is the wave amplitude (including phase) in meters,  $\omega$  is the wave frequency in radians per second,  $K$  is the wave number in 1/m, and  $\theta$  is the direction of the incoming wave. In an irregular sea state, the surface elevation can be described as the contribution from each individual wave:

$$\zeta(x, y, t) = \text{Re} \left( \sum_{m=1}^{\Theta} \sum_{k=1}^N A_{k,m} e^{j(\omega_k t - K_k(x \cos(\theta_m) + y \sin(\theta_m)))} \right) \quad (6)$$

The indices  $m$  and  $k$  represent the wave direction and frequency component, respectively. The method of determining the individual wave components from a given wave spectrum is discussed in the following sections.

### 2.1. Frequency Spectrum Discretization

Several publications discuss the different approaches to discretize a wave spectrum (e.g., [4,5]). Depending on the way the frequency domain is discretized, the methods can be divided into **constant frequency** or a **nonconstant** frequency step. When using a constant frequency step, to obtain a unique

wave elevation time series the number of individual frequency components is obtained from the desired length of the wave time-series. This is obtained from the sampling theorem:

$$N = \frac{2\pi}{\Delta t \Delta \omega} = \frac{t_{max}}{\Delta t} = \frac{2\omega_{max}}{\Delta \omega} \quad (7)$$

Despite the larger number of individual frequency components required, this approach allows the use of computationally efficient fast Fourier transform (FFT) routines. This approach is implemented in FAST for unidirectional seas and was selected for this paper.

A nonconstant frequency step discretization allows the number of frequency components to be reduced while still achieving a unique time-series. The reduced number of frequency components allows the summations in Eq. (6) to be directly computed. This approach is employed by the numerical code OrcaFlex [6] in combination with an equal-energy discretization routine.

### 2.2. Directional Spectrum Discretization

Similar to the frequency spectrum, the directional spectrum can also be subdivided into constant or nonconstant directional steps. When using constant direction steps, two methods of computing the wave elevation in directional sea states are found in the literature: the **double-sum** and **single-sum** methods [7]. A third method involving an **equal-energy discretization** of the directional spectrum is also used in this paper [6]. These are described in the following sections. Here, the wave amplitude is assumed to be deterministic with a random phase; the equations can be extended so that the amplitudes are also randomly distributed (an option available in FAST).

#### 2.2.1. Double-Sum Method

In the double-sum method, the wave spectrum is expressed as a two-dimensional matrix with size  $N$  by  $\Theta$ , where  $N$  is the number of frequency components and  $\Theta$  is the number of directions considered. Therefore, this discretization contains several wave components with the same frequency over different directions. The wave elevation in this case is expressed as in Eq. (6) with the complex wave amplitude given by:

$$A_{k,m} = \sqrt{2S(\omega_k)\Delta\omega} \cdot \sqrt{D(\theta_m)\Delta\theta} \cdot e^{j2\pi U_{k,m}} \quad (8)$$

where  $U_{k,m}$  represents a random number uniformly distributed between  $[0,1]$ , obtained to give a random phase to each wave component with frequency  $\omega_k$  and direction  $\theta_m$ .

#### 2.2.2. Single-Sum Method

The single-sum method avoids having different wave components with the same frequency by subdividing each wave frequency band into subfrequencies  $\Delta\omega' = \Delta\omega/\Theta$ . Therefore, the wave spectrum is expressed as a single vector of dimensions  $N \times \Theta$ , ensuring that the same wave frequency component does not repeat itself along the spectrum. References [8] and [1] suggest uniformly distributing the directions in ascending order across the subfrequencies. This should give the maximum frequency difference between waves

with the same direction. This method is presented in detail in [9]. The wave elevation is in this case expressed by:

$$\zeta(x, y, t) = \text{Re} \left( \sum_{k=1}^{N/\Theta} A_k e^{j(\omega'_k t - K_k(x \cos(\theta_k) + y \sin(\theta_k)))} \right) \quad (9)$$

where  $\omega'_k$  is the subdivided frequency vector. The wave amplitude is obtained using:

$$A_k = \sqrt{2S(\omega_k)\Delta\omega'}. \sqrt{D(\theta_k)\Delta\theta}. e^{j2\pi U_k} \quad (10)$$

The distribution of wave directions  $\theta_k$  is formally given by:

$$\theta_k = \theta_{min} + \Delta\theta k' \text{ with } k' = k \text{mod}(\Theta) \quad (11)$$

where  $\text{mod}(\Theta)$  represents the arithmetic modulo  $\Theta$ . This notation is often used in modular arithmetic function (or clock arithmetic) [10].

The time series obtained with this method will have  $N \times \Theta$  points instead of just  $N$  points. However, only the first  $N$  points are used in the time-domain analysis (because  $t'_{max} = t_{max}\Theta$ ).

### 2.2.3. Equal-Energy Method

The last approach proposed in this paper is to discretize the directional spectrum using an equal-energy method. This is used in the commercial code OrcaFlex [6]. The idea behind this method is to use the same  $N$  points used in the unidirectional case. The equal-energy approach means that each direction component represents the same energy. The discrete amplitude  $A_k$  is kept constant; therefore, the spectrum shape is achieved by using a nonconstant  $\Delta\theta$ . The equal-energy discretization guarantees that there will be more direction components close to the mean wave direction.

The method to determine the distribution of the discrete direction values can be summarized as:

1. Compute the spreading function  $D(\theta)$  for a high number of equally spaced directions  $\theta$  between  $-\theta_{max} < \theta < \theta_{max}$  (blue line in Figure 2).
2. Compute the cumulative energy distribution  $P(\theta) = \int_{-\theta_{max}}^{\theta} D(\theta') d\theta'$  (green line on Figure 2)[5].
3. Calculate the energy step vector, based on the user-defined number of directions  $\Theta$  from  $1/2\Theta$  to  $1 - 1/2\Theta$  (the midpoints of each bin), with a step of  $1/\Theta$  (circles on Figure 2).
4. Interpolate the vector  $P(\theta)$  to get the desired energy steps and determine the discrete values of  $\theta'$  (crosses on Figure 2).

This approach should guarantee that the energy content in the frequency spectrum, discretized by a constant frequency step, is kept constant (eq. (4)) when using multidirectional waves. The wave elevation is given by:

$$\zeta(x, y, t) = \text{Re} \left( \sum_{k=1}^N A_k e^{j(\omega_k t - K_k(x \cos(\theta_k) + y \sin(\theta_k)))} \right) \quad (12)$$

where the wave amplitude is simply given by:

$$A_k = \sqrt{2S(\omega_k)\Delta\omega}. e^{j2\pi U_k} \quad (13)$$

For each frequency sample, one of the discrete directions obtained with the equal-energy approach should be randomly assigned. However, it should be ensured that each discrete direction should be used  $N/\Theta$  times over the frequency spectrum. Therefore, it has to be ensured that  $N/\Theta$  is an integer.

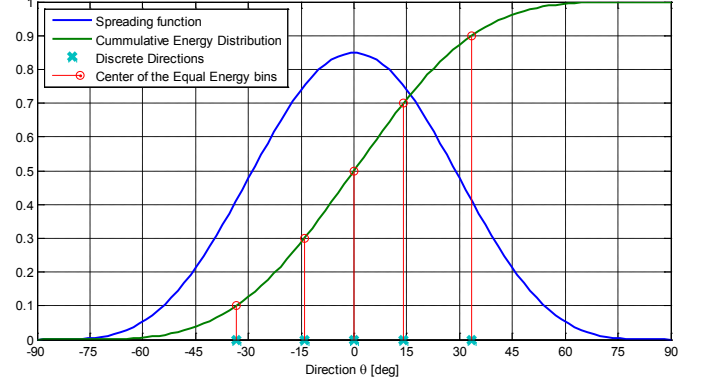


Figure 2. Spreading function, cumulative energy function, and discrete points ( $\Theta = 5$ ).

## 3. COMPARISON OF THE DIFFERENT DISCRETIZATION METHODS

To compare the three methods, the wave elevation and first-order loads were computed for a JONSWAP spectrum with  $H_s = 6$  m and  $T_p = 10$  s and  $\gamma = 2.2$ . The directional spectrum was obtained with Eq. (2), with a spreading coefficient of  $s = 1$  and evaluated between  $-90$  and  $90$  degrees. For the double- and single-sum methods, 40 discrete directions were selected to suitably cover the wave direction spectrum, as recommended in [7]. However, for the equal-energy method, only 10 directions were necessary. This is further discussed in Section 3.4. The wave amplitude was obtained using a deterministic amplitude with a random phase. The unidirectional case is included for comparison purposes.

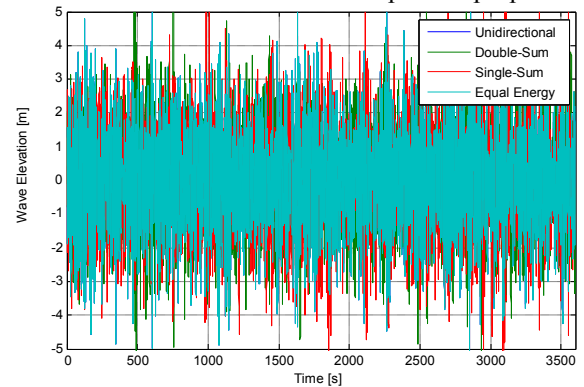


Figure 3. Wave elevation using the different methods.

### 3.1. Wave-Elevation Time Series

The wave elevation at the origin was obtained with all three methods. Figure 3 presents the wave elevation time series at the origin  $(x, y) = (0, 0)$ . Because a random phase was used for each wave component, the time series do not exactly match

between any of the methods except for the equal-energy method. In this case, the time series exactly matches the unidirectional case, as the phase was kept the same and only the wave direction of each frequency component was changed.

The wave spectra can be seen in Figure 4, obtained by performing an FFT routine on the wave-elevation time-series using  $N$  points. The unidirectional case and the equal-energy method provide a smooth line as a result of the constant amplitude, random-phase spectrum used. The double-sum method presents a random amplitude spectrum because of the interaction of the different wave components with the same frequency and different directions and random phases. The single-sum method, despite having just one direction per frequency component, also produces this random amplitude spectrum, as only the first  $N$  points are used from the  $N \times \Theta$  long time-series. The interaction between the different wave components is therefore artificially introduced.

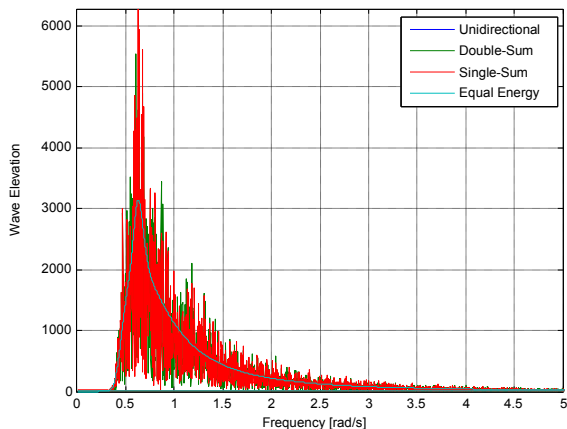


Figure 4. Wave elevation spectra obtained with the different methods.

### 3.2. First-Order Loads

The first-order wave-excitation loads were calculated using the three presented methods. Table 1 presents the equations used to compute the wave loads for the different methods previously described, assuming the reference point of the vessel has coordinates  $(x, y) = (0, 0)$ . The linear transfer function used is representative of the semisubmersible platform studied within the International Energy Agency (IEA) Wind Task 30 Offshore Code Comparison Collaboration Continuation (OC4) project [11].

Table 1. Computation of first-order loads.

Method	First-Order Loads
Double-Sum	$F^{(1)}(t) = \text{Re} \left( \sum_{m=1}^{\Theta} \sum_{k=1}^N A_{k,m} X(\omega_k, \theta_m) e^{j(\omega_k t)} \right)$
Single-Sum	$F^{(1)}(t) = \text{Re} \left( \sum_{k=1}^{N\Theta} A_k X(\omega'_k, \theta_k) e^{j(\omega'_k t)} \right)$
Equal-Energy	$F^{(1)}(t) = \text{Re} \left( \sum_{k=1}^N A_k X(\omega_k, \theta_k) e^{j(\omega_k t)} \right)$

Figure 5 presents the time series for the force calculation in surge and sway. As a result of the random phase discussed earlier, none of the time series exactly match. For the unidirectional case, the sway forces are zero as expected, as the mean wave direction was assumed to be zero degrees.

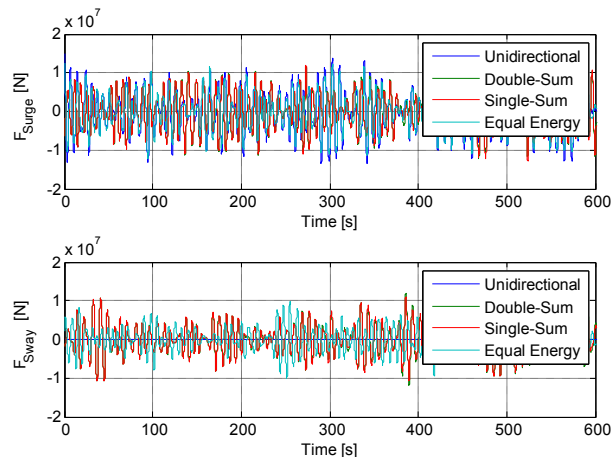


Figure 5. First-order excitation forces in surge (top) and sway (bottom) for the different methods.

Figure 6 presents the spectrum of the force time series. The single-sum and double-sum methods present a random amplitude spectrum because of the obtained random amplitude wave spectrum. The equal-energy method presents a much smoother spectrum. As it only considers a discrete number of directions, and most of them are close to the mean wave direction, all of the directional components have similar contributions to the force in the surge degree of freedom. The sway is smaller than the surge force as expected. The obtained spectrum for the equal-energy method now also presents random amplitude, according to the random direction assigned.

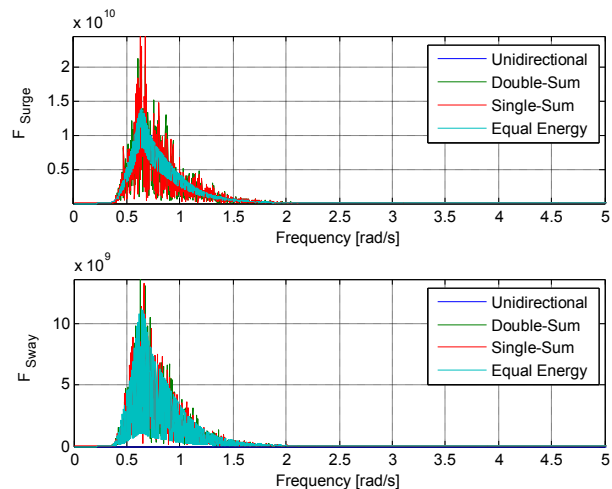


Figure 6. Spectra of the first-order excitation forces for surge (top) and sway (bottom).

Figure 7 presents the ratio of computational time for the different methods compared with the unidirectional case, for a 3,600-s simulation. The equal-energy method used 10 discrete directions, whereas the other methods used 40. The single-sum method presents the highest total value (around 550 times higher than the unidirectional case), as a result of the interpolation of the frequency spectrum, which generates a vector with approximately 1.44 million entries. The equal-energy method is faster than the double-sum method. This difference should be much larger in the computation of the second-order forces.

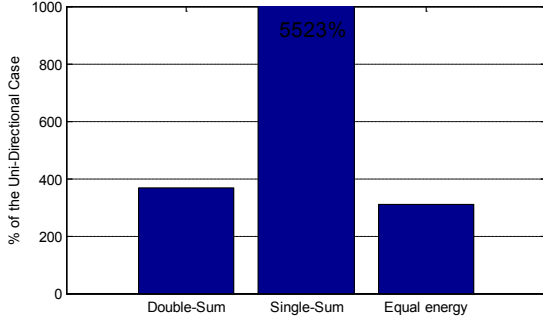


Figure 7. Computational time required for the different methods.

### 3.3. Second-Order Loads

Second-order wave loads require the computation of quadratic transfer functions, both for the difference- and the sum-frequency problems (respectively represented by  $X^-$  and  $X^+$ ). For multidirectional sea states, these matrices are four-dimensional, taking into account the second-order interactions between waves with different frequencies and directions.

Table 2. Computation of second-order loads.

Method	Second-Order Loads
Double-Sum	$F^{(2)}(t) = \text{Re} \left( \sum_{n=1}^{\Theta} \sum_{m=1}^{\Theta} \sum_{k=1}^N \sum_{l=1}^N [A_{k,m} A_{l,n} X^+(\omega_k, \omega_l, \theta_m, \theta_n) e^{j(\omega_k + \omega_l)t} + A_{k,m} A_{l,n}^* X^-(\omega_k, \omega_l, \theta_m, \theta_n) e^{j(\omega_k - \omega_l)t}] \right)$
Single-Sum	$F^{(2)}(t) = \text{Re} \left( \sum_{k=1}^{N\Theta} \sum_{l=1}^{N\Theta} [A_k A_l X^+(\omega'_k, \omega'_l, \theta_k, \theta_l) e^{j(\omega'_k + \omega'_l)t} + A_k A_l^* X^-(\omega'_k, \omega'_l, \theta_k, \theta_l) e^{j(\omega'_k - \omega'_l)t}] \right)$
Equal-Energy	$F^{(2)}(t) = \text{Re} \left( \sum_{k=1}^N \sum_{l=1}^N [A_k A_l X^+(\omega_k, \omega_l, \theta_k, \theta_l) e^{j(\omega_k + \omega_l)t} + A_k A_l^* X^-(\omega_k, \omega_l, \theta_k, \theta_l) e^{j(\omega_k - \omega_l)t}] \right)$

These transfer functions can be obtained in the frequency domain with a second-order panel code, like WAMIT [12]. Table 2 presents the required equations to compute these loads. As can be seen, the double sum-method now requires a

quadruple sum over two directions and two frequencies. The efficiency of the equal-energy approach is very valuable when studying these loads. For this paper, it was not possible to obtain the required transfer functions, and therefore the analysis of these loads will be included in further study. The importance of the second-order loads under multidirectional sea states has been highlighted in [13].

### 3.4. Ergodicity

Ocean waves are usually assumed to be a random ergodic process (stationary and homogenous). The spatial variability is the phenomenon most affected by the different methods used to synthesize multidirectional seas. It has been discussed in the literature how the double-sum method affects the mean wave energy across the domain because of the interaction of waves with the same frequency and different directions [14]. The other important quantity is the variability of the cross-spectrum between two points in space. This quantity is used to determine bidirectional spectra in measurements both in the tank and in the ocean.

#### 3.4.1. Mean Energy

The ergodicity assumption requires that the mean energy across the sea surface is constant. In real sea conditions, this is only untrue in the presence of significant reflected waves, mainly close to shore. In a wave tank, significant reflection can occur depending on the tank configuration and the synthesized waves. However, the energy content should still be constant along the tank. The mean energy can be obtained integrating the energy spectrum for each location [15]:

$$\bar{E} = \rho g \int_0^{\infty} \int_0^{2\pi} S(\omega, \theta) d\theta d\omega \quad (14)$$

Or in the discrete form:

$$\bar{E} = \frac{1}{2} \rho g \overline{|Z(\omega_k)|^2} \quad (15)$$

where  $Z(\omega_k) = A_k N/2$ . To compare the discretization methods, the mean wave energy was computed for a square grid of 1 km by 1 km, in intervals of 10 m. The single-summation and equal-energy methods provided constant energy content across the domain. However, for the double-summation method, we obtained the pattern seen in Figure 8. This result is consistent with the one found in [14].

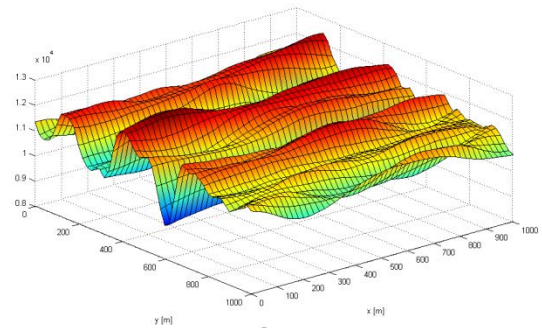


Figure 8. Mean wave energy across the domain for the double-sum method.

As stated in [1], the only way to reduce this variability is to increase the length of the simulation or by averaging different realizations. Figure 9 presents the normalized wave energy for different simulation lengths. The energy content varies within a 5% range for all the realizations, and it is only reduced to 1% for simulations with 9 hours. The variability is not that high because the mean energy is computed for the entire frequency range. Reference [1] presents results for a smaller frequency band, where a variability of up to 60% along the domain was encountered for the shorter simulations.

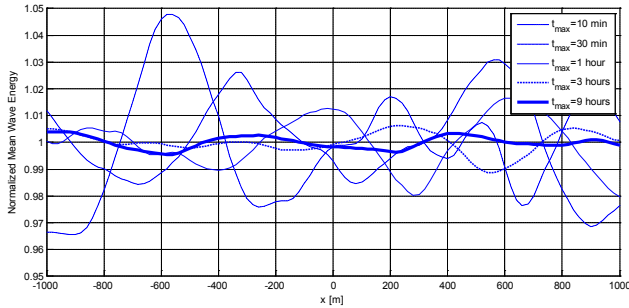


Figure 9. Normalized mean wave energy for the double-sum method and different lengths of the simulation.

One parameter that needs to be taken into account for the single-summation method is the number of directions considered. This value needs to ensure a good discretization, especially close to the peak region of the directional spectrum (close to the mean wave direction). The directional step should be sufficiently small to guarantee that the energy content of the mean wave direction is captured, and this is especially critical for peaked spectrum (high values of the spreading coefficient). Figure 10 shows the mean wave energy for the single-sum method and the equal-energy method. The single-sum method seems to have converged for a number of directions higher than 15. It should be noted that [1] and [14] suggest that a minimum number of 32 directions should be used to guarantee the accuracy of this method, based on the cross-spectrum analysis. The equal-energy discretization guarantees a constant mean wave energy along the domain even when using just two discrete directions.

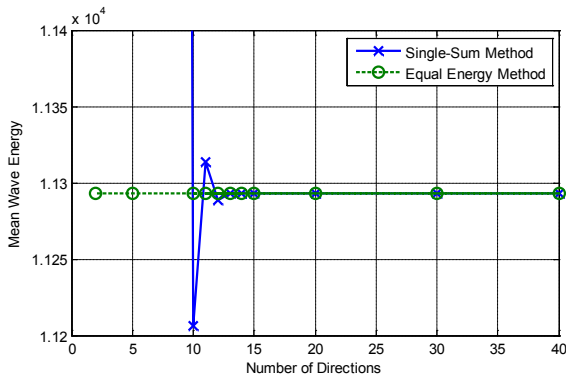


Figure 10. Mean wave energy for the single-sum and the equal-energy method.

### 3.4.2. Cross-Spectrum

The cross-spectrum between the wave elevations at different locations is used to measure wave directionality in wave basins. This section presents the variability of the cross-spectrum between two points. The cross-spectrum between two points  $p$  and  $q$  is given by [4]:

$$S_{pq}(\omega) = \frac{Z_p^*(\omega)Z_q(\omega)\Delta t}{\pi N} \quad (16)$$

Across the domain, the ergodicity assumption requires that the variability is constant along the domain:

$$Var(S_{pq}(\omega)) = Var\left(\frac{Z_p^*(\omega)Z_q(\omega)\Delta t}{\pi N}\right) = const. \quad (17)$$

Figure 11 presents the variance of the cross-spectrum relative to the origin of the referential for the double-sum method. As shown there is a significant variance along the domain, despite using a 3-hr simulation time.

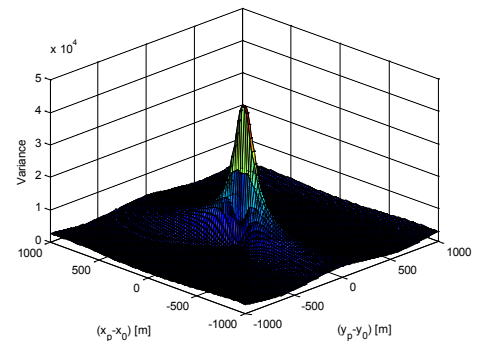


Figure 11. Variance of the cross-spectrum obtained with the double-sum method.

Figure 12 shows the same result for the single-sum and equal-energy method. Despite not being exactly constant across the domain because of numerical issues, the difference across the domain is smaller than 1%.

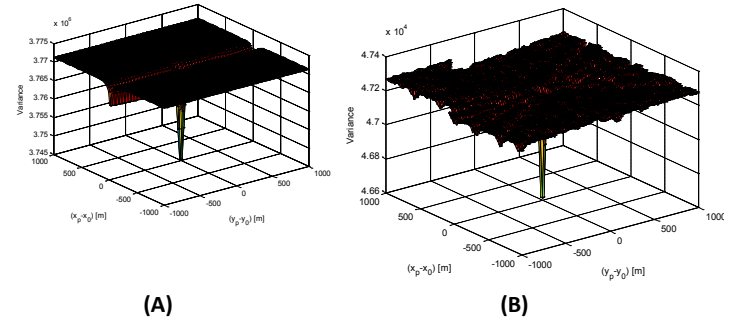


Figure 12. Variance of the cross-spectrum obtained with the single-sum method (A) and equal-energy method (B).

These results are compared along the line  $y = 0$ , in Figure 13, normalized by the mean value of the variance cross-spectrum. Once again it can be seen that the double-sum method does not provide a homogeneous and ergodic sea state.

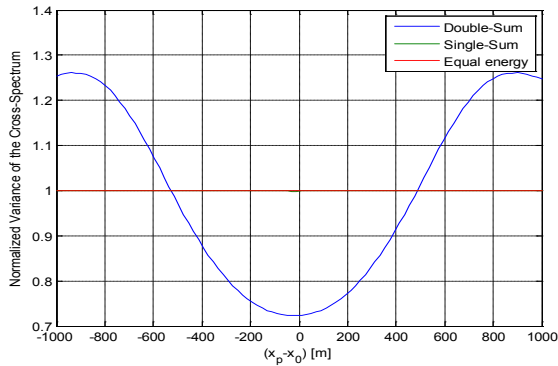


Figure 13. Variance of the cross-spectrum along  $y = 0$  for the different methods.

#### 4. PRELIMINARY ANALYSIS OF A FLOATING OFFSHORE WIND TURBINE UNDER MULTIDIRECTIONAL SEAS

The OC4 semisubmersible platform with the National Renewable Energy Laboratory's 5-MW reference offshore wind turbine was considered for this study [11]. The platform consists of three columns plus a central column where the tower is located, as seen in Figure 14.

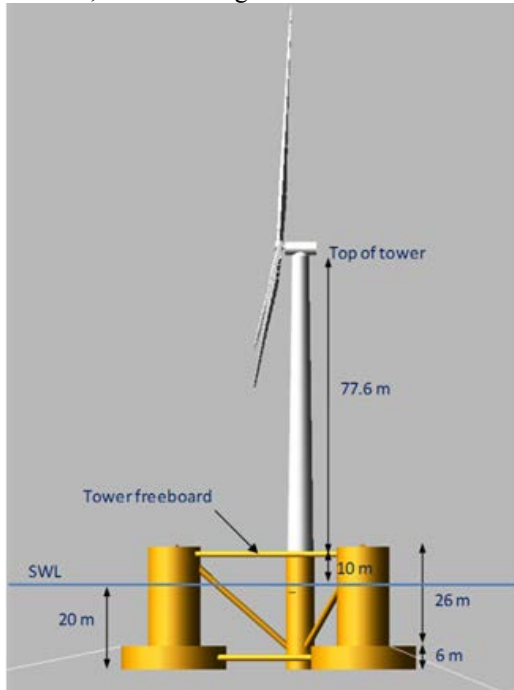


Figure 14. OC4 semisubmersible platform.

The equal-energy method was selected for this analysis. The first-order wave-excitation loads were calculated in MatLab and fed to FAST, which performed the time-marching simulation. The load case chosen corresponds to the JONSWAP spectrum previously mentioned. A spreading coefficient of one was selected for the multidirectional case. No wind loads were considered in this analysis.

Figure 15 presents the platform motions for this case, with a unidirectional sea state and a multidirectional case. For both cases, the main wave direction is aligned with the  $x$ -axis of the platform, which represents the surge motion.

As expected, the platform has basically no sway and roll motion in the unidirectional sea. However, for the multidirectional case, there is a significant additional motion of the platform in these degrees of freedom. The sway and roll motion found represents roughly 20% of the surge and pitch motion, respectively.

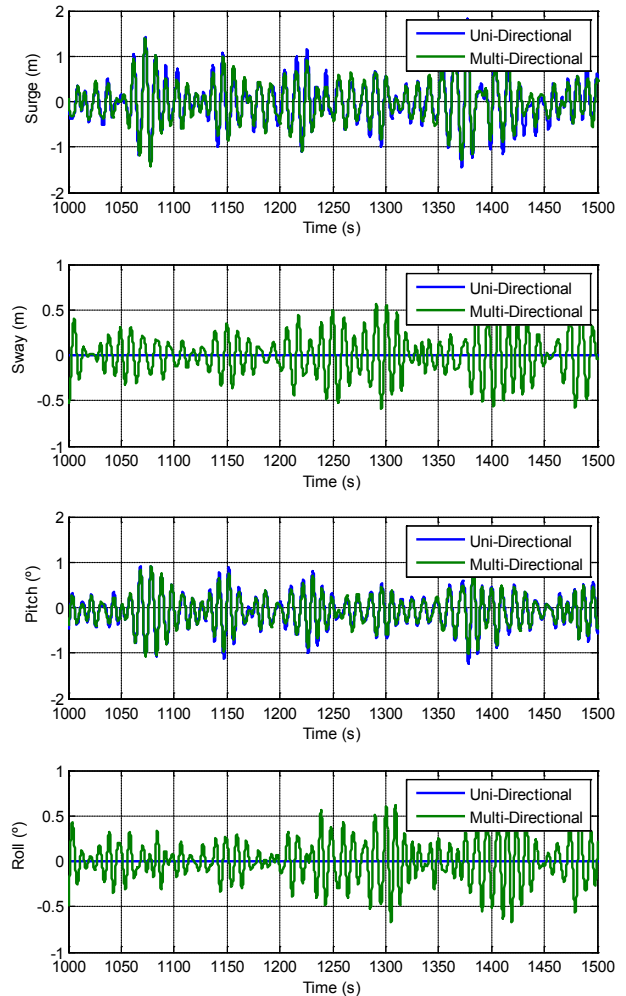


Figure 15. Platform motions under irregular sea state, with and without multidirectional loading.

#### 5. CONCLUSIONS

In this paper we reviewed different methods to synthesize the wave elevation under multidirectional sea states. The double-sum method is the most commonly mentioned method in the literature, but does not provide an ergodic solution. The single-sum method fixed this problem, by shifting the different frequency components and avoiding the interaction between them. However, it still requires significant computational time, especially for long simulations. The equal-energy method described here combines a constant frequency-step

discretization with an equal-energy discretization of the directional spectrum. This allows using the same number of frequency components for both the unidirectional and multidirectional cases, thus saving significant computational effort. This method also proved to ensure the ergodicity properties of the wave spectrum. Based on these results, this method was selected to be implemented within FAST and should become available in a future release.

In addition, a preliminary study was performed on the OC4 semisubmersible platform. The comparison between the unidirectional and multidirectional sea state without wind loads showed a significant increase in the platform sway and roll motion. These findings should motivate further studies to carefully assess the impact of the multidirectional loads on the platform's ultimate loads and fatigue life.

## 6. ACKNOWLEDGMENTS

This work was supported by the U.S. Department of Energy under Contract No. DE-AC36-08-GO28308 with the National Renewable Energy Laboratory.

## 7. REFERENCES

- [1] Miles, M. D., and Funke, E. R., 1989, "A Comparison of Methods for Synthesis of Directional Seas," *JOMAE*, **111**(1), pp. 43-48.
- [2] Alves, M., 2012, "Numerical Simulation of The Dynamics of Point Absorber Wave Energy Converters Using Frequency and Time Domain Approaches," Ph.D. Thesis, Instituto Superior Tecnico. Lisboa, Technical University of Lisbon.
- [3] WAFO-group, 2000, "A MatLab Toolbox for Analysis of Random Waves and Loads - A Tutorial," Lund, Sweden: Center for Math. Sci., Lund Univ.
- [4] Kim, C. H., 2008, "Nonlinear Waves and offshore Structures," World Scientific Publishing Co. Pte. Ltd., Singapore.
- [5] Goda, Y., 2000, "Random Seas and Design of Maritime Structures," World Scientific Publishing Co. Pte. Ltd., Singapore.
- [6] Orcina, 2012, "OrcaFlex Manual – Version 9.6."
- [7] Miles, M. D., Benoit, M., Frigaard, P., Hawkes, P. J., Schäffer, H. A., and Stansberg, C. T., 1997, "A Comparison Study of Multidirectional Waves Generated in Laboratory Basins," Proceedings of the 27th IAHR Congress, San Francisco. IAHR Seminar: Multidirectional Waves and Their Interaction with Structures.
- [8] Pascal, R., and Bryden, I., 2011, "Directional Spectrum Methods for Deterministic Waves," *Ocean Engineering*, **38**(13), pp. 1382–1396.
- [9] Pascal, R., 2012, "Quantification of the Influence of Directional Sea State Parameters over the Performances of Wave Energy Converters," The University of Edinburgh, Edinburgh.
- [10] Insall, M., and Weisstein, E. W., "Modular Arithmetic." From MathWorld--A Wolfram Web Resource. [Online] 2012. [Cited: 03 07, 2013.] <http://mathworld.wolfram.com/ModularArithmetic.html>.
- [11] Robertson, A., Jonkman, J., Masciola, M., Song, H., Goupee, A., Coulling, A., and Luan, C., "Definition of the Semisubmersible Floating System for Phase II of OC4," to be published as NREL Technical Report, 2014.
- [12] WAMIT Inc. [Online] <http://www.wamit.com/>.
- [13] Waals, O. J., 2009, "The Effect of Wave Directionality on Low Frequency Motions and Mooring Forces," Honolulu, Proceedings of the 28th International Conference on Ocean, Offshore and Arctic Engineering - OMAE2009.
- [14] Jefferys, E. R., 1987, "Directional Seas Should Be Ergodic," *Applied Ocean Research*, **9**(4), pp. 186-191.
- [15] Newman, J. N., 1977, *Marine Hydrodynamics*, MIT Press, Cambridge, chapter 6.